



저작자표시-비영리-변경금지 2.0 대한민국

이용자는 아래의 조건을 따르는 경우에 한하여 자유롭게

- 이 저작물을 복제, 배포, 전송, 전시, 공연 및 방송할 수 있습니다.

다음과 같은 조건을 따라야 합니다:



저작자표시. 귀하는 원저작자를 표시하여야 합니다.



비영리. 귀하는 이 저작물을 영리 목적으로 이용할 수 없습니다.



변경금지. 귀하는 이 저작물을 개작, 변형 또는 가공할 수 없습니다.

- 귀하는, 이 저작물의 재이용이나 배포의 경우, 이 저작물에 적용된 이용허락조건을 명확하게 나타내어야 합니다.
- 저작권자로부터 별도의 허가를 받으면 이러한 조건들은 적용되지 않습니다.

저작권법에 따른 이용자의 권리는 위의 내용에 의하여 영향을 받지 않습니다.

이것은 [이용허락규약\(Legal Code\)](#)을 이해하기 쉽게 요약한 것입니다.

[Disclaimer](#)

Cell tracking by magnetic resonance imaging using ferritin in atherosclerosis and cancer mouse models

Chan Wha Lee

Department of Medicine

The Graduate School, Yonsei University

Cell tracking by magnetic resonance imaging using ferritin in atherosclerosis and cancer mouse models

Directed by Professor Jin-Suck Suh

The Doctoral Dissertation
submitted to the Department of Medicine,
the Graduate School of Yonsei University
in partial fulfillment of the requirements for the degree of
Doctor of Philosophy

Chan Wha Lee

June 2016

This certifies that the Doctoral Dissertation
of Chan Wha Lee is approved.

Thesis Supervisor: Jin-Suck Suh

Thesis Committee Member#1: In-Hong Choi

Thesis Committee Member#2: Sahng Wook Park

Thesis Committee Member#3: Goo Taeg Oh

Thesis Committee Member#4: Daehong Kim

The Graduate School
Yonsei University
June 2016

ACKNOWLEDGEMENTS

Foremost gratitude goes to Professor Jin-Suck Suh, who has been a dedicated and inspirational figure throughout my PhD studies.

Even though there were difficult moments when experiments did not go as planned or took longer than expected, and when the end seemed to be out of reach, I thank Dr. Daehong Kim and Dr. Yun-Hee Kim who looked out for me in these times with their unhesitating offers of encouragement and help.

I also thank committee members Dr. In-hong Choi, Dr. Sahng Wook Park, Dr. Goo Taeg Oh, and Dr. Daehong Kim for their unending patience, for always kindly offering their assistance however tight the schedule was.

My gratitude also goes to Dr. Joo-Hyuk Lee for directing my interest towards molecular imaging and for giving me a firm but encouraging hand that kick-started my PhD studies.

Finally, my greatest thanks go to my husband and sons Kyung Suh and Kyung Jay, for having given me all their love, support, and encouragement that have kept me going throughout my studies.

<TABLE OF CONTENTS>

ABSTRACT	1
I. INTRODUCTION	4
II. MATERIALS AND METHODS	7
1. Cell culture	7
2. Ferritin	7
3. Preparation of cell pellets for <i>in vitro</i> MR imaging	7
4. Animal models and preparation	8
5. MR hardware and imaging parameters	10
6. Prussian blue staining	11
III. RESULTS	12
1. R2-relaxivity of ferritin	12
2. Images with <i>ApoE</i> ^{-/-} mouse	12
3. Macrophage imaging with ferritin in atherosclerosis model	15
4. MR imaging of macrophage with ferritin in cancer model	17
5. Ferritin as a reporter for MR imaging in cancer mouse model	19
IV. DISCUSSION	24
V. CONCLUSION	27
REFERENCES	28
ABSTRACT(IN KOREAN)	31

LIST OF FIGURES

Figure 1. T2 maps of Feridex and ferritin for measurement of relaxivity	13
Figure 2. MRI of an untreated <i>ApoE</i> ^{-/-} mouse for evaluation of the aortic arch	14
Figure 3. <i>In vitro</i> and <i>in vivo</i> images of ferritin-labeled macrophages	16
Figure 4. MRI of macrophages labeled with ferritin in a colon cancer cell model	18
Figure 5. MRI of ferritin as a reporter in a HCT116 subcutaneous tumor model	20
Figure 6. Ferritin-induced MR contrast effect <i>in vitro</i> in U87MG cells	21
Figure 7. Brain MR images in a glioma mouse model infected with Ad-hFTH	22
Figure 8. Serial MRI of a glioma with Ad-hFTH	23

ABSTRACT

Cell tracking by magnetic resonance imaging using ferritin in atherosclerosis and cancer mouse models

Chan Wha Lee

*Department of Medicine
The Graduate School, Yonsei University*

(Directed by Professor Jin-Suck Suh)

Molecular imaging is a type of innovative medical imaging that provides detailed images of the *in vivo* occurrences at a molecular or cellular level through real-time imaging. Among the various molecular imaging modalities, magnetic resonance imaging(MRI) can use in detection of cell movement, proliferation, and division through cell labeling, and diagnose and evaluate the treatment effectiveness of tumors or inflammations depending the labeling cell type. MRI provides high tissue contrast and superior resolution but it has relatively low sensitivity, and therefore, contrast agents are used to overcome this challenge. However, problems such as dilution of contrast agents within the body, instability of cell labeling, and cytotoxicity suggest that there is a need for a more safe and efficient cell labeling technique. The reporter-gene based technique is being proposed as a method to overcome these problems. Ferritin is an intracellular, iron-binding protein that accumulates extracellular iron entering the cell and exhibits magnetic properties, allowing T2 contrast effects

under MRI. This makes it a good candidate as an MR contrast agent for cell tracking. This study aims to understand the effectiveness of ferritin as a contrast agent and also a potential reporter gene, by tracking macrophages and tumor cells using ferritin in arteriosclerosis and tumor mouse models. In a comparison experiment with the currently used T2 contrast agent Feridex, ferritin showed 50% lower relaxivity (Feridex vs ferritin = $0.00298 \text{ ml}/\mu\text{g Fe} \cdot 1/\text{sec}$ vs $0.00159 \text{ ml}/\mu\text{g Fe} \cdot 1/\text{sec}$), which was sufficient to act as the MR contrast agent for cellular imaging. Macrophage cell line Raw264.7, labeled with ferritin, showed T1 and T2 contrast effects in cell pellet imaging. *In vivo* imaging of ApoE knockout (*ApoE*^{-/-}) mice 24 hr after intravenous injection of the cells revealed negative contrast effects in the aortic arch walls. Therefore, ferritin can be used to diagnose inflammations by tracking ferritin-labeled macrophages. Since the contrast effects of ferritin were confirmed, the use of ferritin as a reporter gene and its use as an adenovirus-based expression system were assessed in this experiment. First, a Mock (control group) and an adenoviral human ferritin heavy chain ([Ad-FTH] experimental group) were injected into the subcutaneous tumor models made using the colorectal cancer cell line HCT116. T1 and T2 -weighted images were obtained every two days after injection. Day 2 post-injection images showed negative contrast areas within the tumor, and by day 4 post-injection, the enhanced contrast areas were clearly observed. The results of the Prussian blue staining performed using the same tissue samples demonstrated overlapping of the negative contrast-enhanced region and iron absorption region, thereby confirming that the contrast effects were due to ferritin gene expression. Considering the fact that the iron concentration increases within the tumor, a glioma cell line U87MG was infected with Ad-FTH and ferritin expression was induced. Then, cell-pellet MRI was performed using cells cultured with 1mM FeCl₃ and 3mM FeCl₃; cells cultured under higher iron concentration were confirmed to show stronger negative

contrast enhancing effects. In order to validate the negative contrast effects of ferritin through T2*-weighted images, brain tumor models were established by injecting U87MG cells into mouse brain and Ad-FTH was injected into the tumor; T1, T2 and T2*- weighted images were simultaneously obtained from days 1 through 6. Day 2 post-injection, T2 and T2*- images showed negative contrast effects at the tumor margins, and maintained until day 6. In conclusion, through cellular level investigation and in vivo experiments using animal models, this study strongly suggests the effectiveness of ferritin as an endogenous MR contrast agent and a potential reporter gene, which is capable of maintaining cell labeling stability and cellular safety.

Key words: ferritin, cell tracking, MR imaging, reporter gene

Cell tracking by magnetic resonance imaging using ferritin in atherosclerosis and cancer mouse models

Chan Wha Lee

*Department of Medicine
The Graduate School, Yonsei University*

(Directed by Professor Jin-Suck Suh)

I. INTRODUCTION

Until recently, medical imaging was mostly based on anatomical imaging. However, to address an increased diagnostic need for information related to functional imaging and metabolism, novel imaging approaches were developed—namely, molecular imaging. The advent of molecular imaging can be attributed as the synergistic outcome of the following factors: the rapidly advancing field of biotechnology encompassing various overlapping fields such as cell biology, genetics, bioinformatics, and proteomics; and the merger between chemistry and nanotechnology.

Molecular imaging differs from indirect experimental approaches or from those that rely on microscopic images. The results of the latter approaches are based on laboratory findings and analyses at the molecular or cellular levels to investigate cellular and pathological phenomena, whereas molecular imaging

provides a more intuitive approach to gaining insight into disease pathophysiology and cellular mechanisms through *in vivo*, real-time imaging^{1,2}. The types of molecular imaging include magnetic resonance imaging (MRI)³⁻⁸, nuclear imaging⁹, and optical imaging¹⁰, and each has its own benefits and limitations. Of these, MRI presents with strong advantages such as showing the highest resolution and tissue contrast, and being a non-invasive imaging approach without exposure to radiation. However, compared to that of nuclear imaging or optical imaging, MRI shows relatively low signal sensitivity¹¹. To increase the sensitivity of MRI, contrast agents such as paramagnetic gadolinium- and super-paramagnetic iron-oxide-based agents have been used. The inhomogeneity and bio-instability of these magnetic particles, which leads to poor signal enhancement, still contributes to the slow growth of molecular imaging technology, however, recent developments in nanotechnology have paved way to its substantial advancement^{12,13}

Molecular MRI includes cell targeting and tracking imaging. The former uses a targeted-probe to diagnose and treat tumors and inflammation, and the latter marks grafted cells so that their movement, proliferation, differentiation, and final fate can be traced for treatment purposes. For cellular MRI, the easiest method is the direct targeting of cells by an MR contrast agent; however, barriers such as dilution and instability of the contrast agents limit the quality of the imaging. Nonetheless, the use of a reporter gene has been shown to moderately increase specificity and allow for long-term labeling of target cells. Studies relating to MRI reporter genes have been undertaken to investigate effective, safe, and more specific imaging methods of cell targeting. However, the MRI reporter genes that have been used thus far including tyrosine, transferrin receptor (TfR)¹⁴, transferrin, and beta-galactosidase have failed to give reproducible MRI results¹⁵. Remarkably, ferritin, a putative MRI reporter

gene, was shown to be associated with a high reproducibility for cellular MRI¹⁶⁻¹⁸.

Ferritin is an intracellular metalloprotein comprising a light and a heavy polypeptide chain and binds to free iron¹⁹. In spite of a low intracellular iron concentration, ferritin is an endogenous nanoparticle that shows a high, intrinsic magnetic property²⁰ that is sustained without the need of an external contrast agent. Thus, ferritin may prove to be a very effective and safe MR contrast agent for cell tracking imaging¹⁸.

This study aims to understand the effectiveness of ferritin as a contrast agent and potential reporter gene, by tracking macrophages and tumor cells using ferritin in mouse models of arteriosclerosis and cancer.

II. MATERIALS AND METHODS

1. Cell culture

All cell lines used in this study were purchased from American Type Culture Collection. RAW264.7, a murine macrophage cell line, was maintained in RPMI medium supplemented with 10% Fetal Bovine Serum (FBS) (Invitrogen, Carlsbad, CA, USA) and 1% penicillin/streptomycin (Invitrogen). U87MG, a human glioblastoma cell line, and HCT116, a human colon cancer cell line, were maintained in DMEM containing 10% FBS and 1% penicillin/streptomycin. All cells were maintained in a humidified incubator at 37°C with 5% CO₂.

2. Ferritin

For labeling of macrophage cells, ferritin from equine spleen was purchased from Sigma-Aldrich Co. (Sigma-Aldrich Co, St. Louis, MO, USA) (cat no. F4503). To verify the function of ferritin as a reporter gene, high-titer adenovirus (2×10^{11} PFU/ml) of Ad5-hFTH was purchased from Vector Biolabs (Vector Biolabs, Malvern, PA, USA). The adenoviral vector was designed so that EGFP expression was able to reflect adenoviral transduction.

3. Preparation of cell pellets for *in vitro* MR imaging.

For measurement of the effect of ferritin-mediated MR contrast in cells, RAW264.7 cells (5×10^6) were incubated with equine ferritin, at a working concentration of 5 mg/ml, in serum-free medium. For U87MG cells, 3×10^6

cells were infected with 2×10^8 PFU adenovirus encoded human ferritin heavy chain (hFTH) and Mock for 48 hr in complete medium containing FeCl_3 at the indicated concentration at 37°C with 5% CO_2 . After incubation, all cells were collected by centrifugation at 2000 rpm and washed with phosphate-buffered saline (PBS) three times. Centrifuged cells were transferred to 0.2 ml thin wall strip tubes, and MRI measurements were taken using the cell pellets.

4. Animal models and preparation for MRI

The animals used in this study were kept under specific-pathogen-free conditions and maintained in a National Cancer Center animal facility in accordance with the AAALAC International Animal Care policy (accredited unit; National Cancer Center Research Institute; unit number 1392). Animal model was performed in accordance with an experimental proposal (No. NCC-10-043C, NCC-11-124).

A. Animal models

(A) Atherosclerosis

Apolipoprotein E-deficient (*ApoE*^{-/-}) mice were provided by Dr. Goo Taeg Oh. *ApoE*^{-/-} mice were fed a diet containing 0.15% cholesterol, 20% fat, and 0.05% sodium cholate (Research Diet Inc., New Brunswick, NJ, USA). After approximately eight months, ferritin-labeled RAW264.7 cells (5×10^6), which had been previously incubated with equine spleen derived ferritin (5 mg/ml) at 37°C in 5% CO_2 for 24hr, were injected intravenously into atherosclerosis-induced mice.

(B) Colon cancer model

HCT116 cells (3×10^6) were subcutaneously injected into the flanks of mice following care for roughly two weeks. The mean tumor volume was roughly 100 mm^3 . To verify the efficiency of ferritin as a reporter gene, mice were intratumorally injected with 5×10^8 PFU of Ad-Mock or Ad-hFTH into each left and right tumor site, respectively. To track macrophages containing ferritin, RAW264.7 cells (5×10^6), previously incubated with equine ferritin (5 mg/ml) for 24hr, were intravenously injected into mice.

(C) Orthotropic glioma model

Six-week-old female BALB/c nude mice were purchased from Central Lab Animal Inc. (Seoul, Korea), and U87MG cells (3×10^6) were intracranially injected into the right brain of mice following care for two weeks with MRI every four to five days. Briefly, 14 days after inoculation with the U87MG cells, the mice were intracranially injected with 2×10^8 PFU of Ad-hFTH into the tumor region.

B. Animal preparation for MRI

The animal was sedated with 1~3% isoflurane through a nose cone. Its core temperature was monitored by a rectal thermistor and maintained at 37°C by a flow of warm air. An electrocardiogram (ECG) was also taken by attaching a pair of sub-dermal needle electrodes. In order to suppress artifacts associated with motion, respiratory motion was monitored using an air pillow

5. MR hardware and imaging parameters

All experiments were performed using a 7T MR scanner (BioSpec 70/20, Bruker, Germany) with T1-, T2- and T2*-weighted imaging techniques. A 35-mm-diameter quadrature birdcage-type RF coil was used for imaging of the aortic arch and subcutaneous cancer. For brain imaging of the model animals, a combination of the four-channel arrayed surface-type receive-only RF coil and 72-mm-diameter transmit-only RF coil was used.

To visualize the aortic arch, a short TE spin echo pulse sequence was applied with fat-suppression and flow-saturation technique. The acquisition parameters used were repetition time (TR) = 500ms; echo time (TE) = 7.1ms; 256×192 acquisition matrix; field of view (FOV) = 4×3 cm; slice thickness = 0.7 mm; delay time after R-peak: 30~80ms. To obtain consistent image-contrast, the heart-rate of the mouse was maintained at approximately 50 beats-per-min by adjusting the isoflurane concentration.

MRI examination was performed for brain cancer model animals, which involved the T1-weighted (T1w) spin echo sequence and T2-weighted (T2w) rapid acquisition with relaxation enhancement (RARE) sequence. Imaging parameters were repetition time (TR) = 800ms (T1w)/2500ms (T2w); echo time (TE) = 10ms (T1w)/35ms (T2w); 256×192 acquisition matrix; field of view (FOV) = 2×2 cm; slice thickness = 0.7 mm; RARE factor = 8. T2*-weighted images were obtained using fast low angle shot (FLASH) sequence with the following acquisition parameters: TR = 200ms; TE = 4ms; the geometry parameters used were the same as above. MR images of glioma mice were obtained before and daily up to six days after injection of Ad-hFTH.

The T1-weighted spin-echo and T2-weighted RARE sequences were performed for imaging the colon cancer model animals. The acquisition

parameters were repetition time (TR) = 700ms (T1w)/2500ms (T2w); echo time (TE) = 10.5ms (T1w)/30ms (T2w); 256×192 acquisition matrix; field of view (FOV) = 2×2 cm; slice thickness = 0.7 mm; RARE factor = 8. MR images of HCT116 tumor model were acquired before, 6 hr and daily after injection of Ad-hFTH. For HCT116 tumor mode with i.v. injection of ferritin-labeled macrophage, MR imaging was performed before and every two days after injection.

6. Prussian blue staining

For analysis of Fe uptake by ferritin, cryosections of colon cancer tissue were fixed with 4% formaldehyde, and then washed with distilled water four times. Before staining, 5% potassium ferrocyanide was mixed with 5% hydrochloric acid at a 1:1 ratio. Fixed specimens were incubated with the mixed solution for 1hr at room temperature, washed with water four times, and counter stained with Fast Red. The slides were scanned using the Aperio Imagescope v10.2.2.2319 software.

III. RESULTS

1. R2-relaxivity of ferritin

In order to examine the relaxivity (R2) of ferritin, MRI scans were performed for several concentrations of ferritin and Feridex with the conventional spin-echo pulse sequence. The signal intensity of the spin-echo images was averaged in the dotted areas (Fig.1). The T2 values of the samples were calculated by fitting with a single exponential function. Using the T2 values, the R2 of ferritin and Feridex was calculated. The R2 of ferritin was measured as 0.00159 ml/ μ g Fe \cdot 1/sec, which is almost half of that of Feridex at 0.00298 ml/ μ g Fe \cdot 1/sec. The R2 value of ferritin is sufficient to act as the MR contrast agent for cellular imaging.

2. Images with *ApoE*^{-/-} mouse

Spin echo T1 weighted sagittal images of the aortic arch were obtained. We used the fat suppression and flow saturation technique for better image quality of the aorta, and adjusted the delay time to reduce the motion artifact (Fig. 2A-D). The image quality was improved with a 30–80ms delay time after the R-peak. TR time was determined by the heart rate of the mouse, and the best image quality of delay time appeared to be 50ms. Since it is problematic to obtain the whole aortic arch in one image slice, the axial plane is better than the sagittal plane to image the plaque of the aortic arch (Fig. 2E).

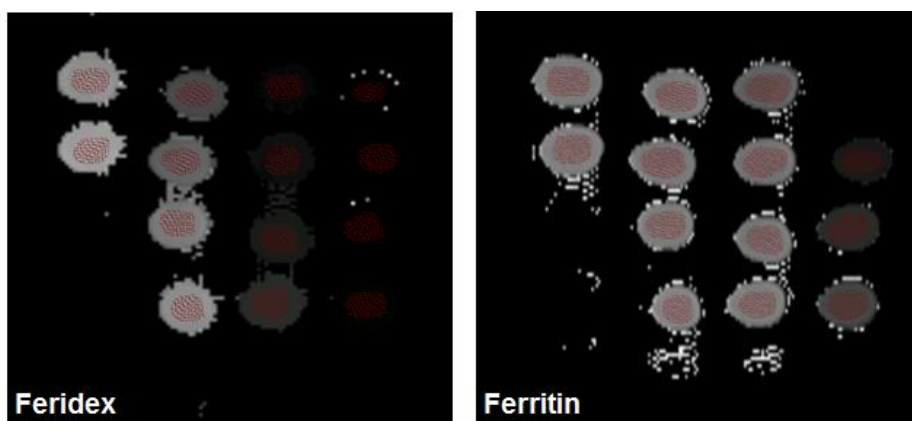


Figure 1. T2 maps of Feridex and ferritin for measurement of relaxivity(R2).

In order to examine the R2 of ferritin, T2-weighted spin-echo images were obtained using various concentrations of ferritin and Feridex. The prepared concentrations of ferritin were 11.1 mg Fe/ml and subsequent continuous 1:2 dilutions. Concentrations of Feridex were 11.2 mg Fe/ml and subsequent continuous 1:2 dilutions. T2 maps for ferritin and Feridex were obtained from T2-weighted spin-echo images of ferritin and Feridex. Using the averaged T2 values in the red-dotted ROIs, the R2 were calculated as 0.00298 ml/ μ g Fe \cdot 1/sec for Feridex and 0.00159 ml/ μ g Fe \cdot 1/sec for ferritin.

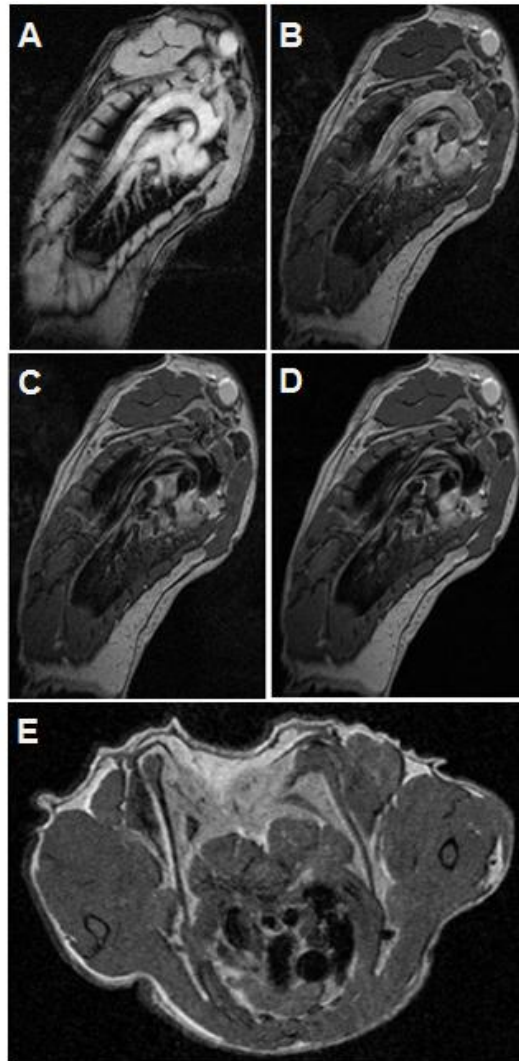


Figure 2. Magnetic resonance images of an untreated *ApoE*^{-/-} mouse for evaluation of the aortic arch. The image parameters were adjusted in order to improve the image contrast of the aortic arch. Oblique slice images of the aortic arch using spin echo pulse sequence (A), fat suppression technique (B), flow saturation (C), and a 50ms delay time (D). The axial spin echo image of an *ApoE*^{-/-} mouse at the level of the aortic arch (E).

3. Macrophage imaging with ferritin in an atherosclerosis model

To examine the contrast effect of ferritin in the atherosclerosis model, RAW264.7 cells were labeled with ferritin (5 mg/ml) and the signal intensity of MR was examined as described in the Materials and Methods. T1 weighted spin echo (TE/TR 6.7/500ms) images of the cell pellets showed dark signal intensity in the pellets of RAW264.7 cells with ferritin contrast compared to that of the control (Fig. 3A). The T2-weighted RARE image (TE/TR 40/200ms) shows dark signal intensity in both groups.

Subsequently, MR imaging of *ApoE*^{-/-} mice injected with ferritin-labeled RAW264.7 cells via their tail vein was performed (Fig. 3B). As compared to the pre-contrast image, the post 1 day image showed loss of intimal signal intensity in the aortic arch. These results suggest that macrophage cells can be identify the in an atherosclerosis model by the negative contrast effect of ferritin-labeling.

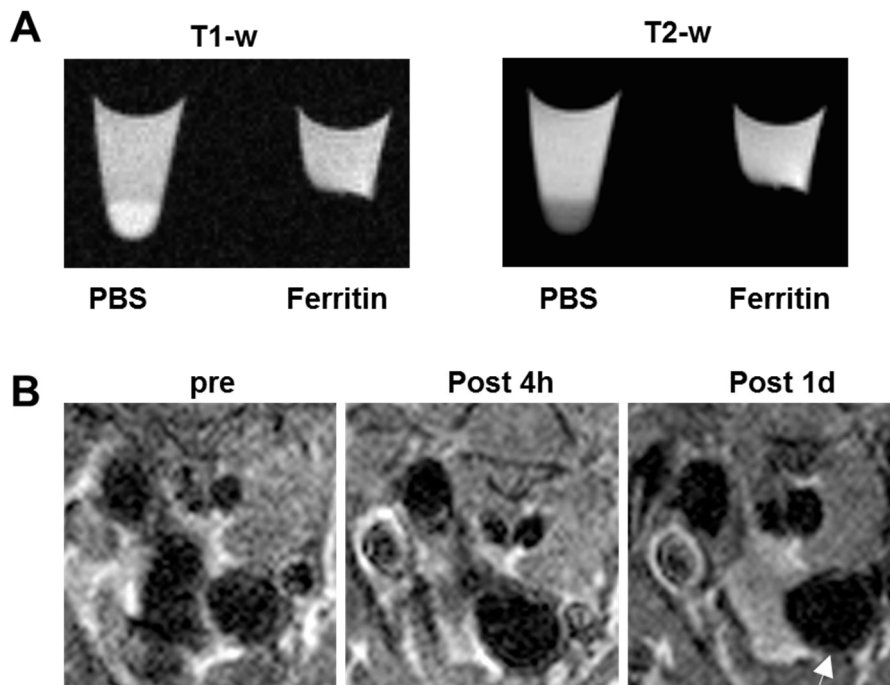


Figure 3. *In vitro* and *in vivo* images of ferritin-labeled macrophages. (A) The macrophage pellets labeled with equine ferritin showed a strong negative enhanced contrast in the conventional T1 & T2-weighted images. To prepare macrophage pellets, RAW 264.7 cells were incubated with culture medium containing equine ferritin (5 mg/ml) for 24hr, and then cells were centrifuged in order to collect them at the bottom of tube. (B) After the injection of macrophages labeled with equine ferritin into an *ApoE*^{-/-} mouse, axial T1 weighted images showed the gradual negative enhancement of signal (arrow) at the aortic arch.

4. MRI of macrophages with ferritin in a cancer model

To validate whether macrophage cells labeled with ferritin are suitable for cancer tracking, *in vivo* MR imaging of ferritin-labeled RAW264.7 cells in a subcutaneous xenograft mouse model using HCT116, a human colon cancer cell line (Fig. 4) was performed. Two days after administration of RAW264.7 cells via intravenous injection, which was performed after the tumor size reached about 100 mm³ at 14 days, MR images of the flank tumor showed a faint dark spot within the tumor mass. The dark spots were increased in number and were more distinct on day 4 post-injection of RAW264.7 cells (Fig. 4B). Next, to confirm the uptake of iron by ferritin, Prussian blue staining of paraffin-embedded tumor sections was performed. Multiple blue dots were observed near vessel structures, suggesting that macrophage cells containing ferritin-mediated iron were distributed (Fig. 4C). These results suggest that ferritin-labeled macrophage cells are effective monitoring tools of tumor utilizing cells with tropism into the tumor

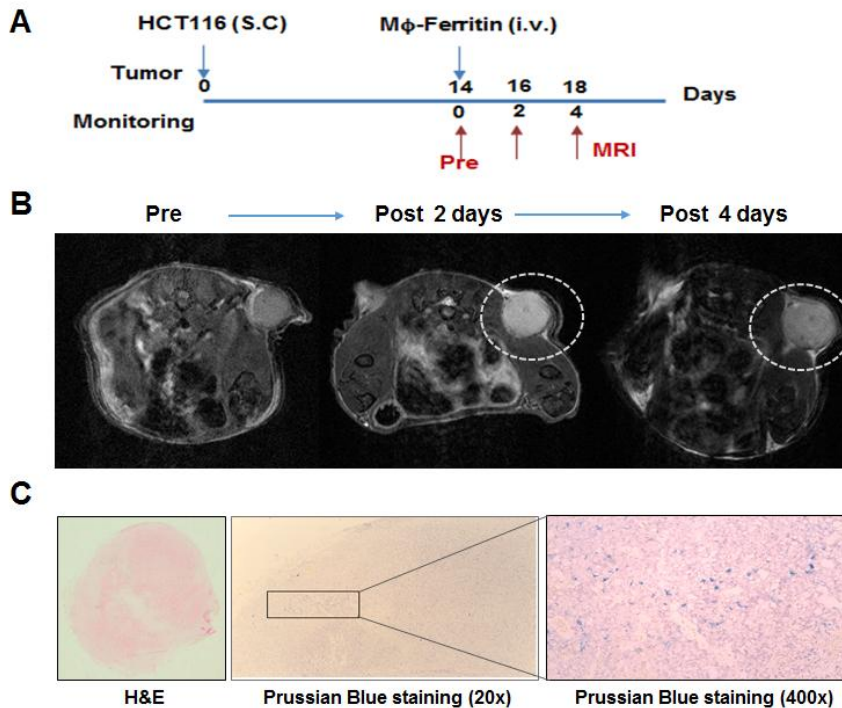


Figure 4. Magnetic resonance imaging (MRI) of macrophages labeled with ferritin in a colon cancer cell model. (A) Experimental scheme of macrophage tracking in a colon cancer cell mouse model using HCT116 cells. RAW264.7 macrophage cells labeled with equine ferritin were administrated intravenously (i.v.) via tail vein after tumor formation 14 days after subcutaneous (S.C) injection of HCT116 colon cancer cells. MR monitoring was performed every two days after acquiring pre-imaging. (B) In T2-weighted axial images, the dark spot inside the tumor mass (white dotted circle) could be observed four days after the injection of the equine ferritin labeled macrophages. (C) Prussian blue staining of the tumor mass showed scattered purple dots suggesting iron uptake in the tumor mass. The staining method is described in the Materials and Methods.

5. Ferritin as a reporter for MRI in a mouse model of cancer

To investigate whether ferritin works as a reporter for MRI, we used the serotype 5 adenoviral expression system of human ferritin heavy chain (Ad-hFTH). A non-replicable adenovirus with a bi-promoter for hFTH and GFP was designed to monitor the transduction efficiency of adenovirus by GFP expression (Fig. 5A-B). First, the ferritin-induced signal intensity was measured in a colon cancer cell mouse model after intratumoral administration of 5×10^8 PFU adenovirus at the indicated time points (Fig. 5C). T2 weighted images of all seven mice showed that low signal intensity within the Ad-hFTH tumor appeared at 6hr post injection, and gradually enlarged at 24 and 48 hr. In five mice (#1, 3, 4, 6, and 7), there was no signal drop in the side of Mock-infected tumor, whereas mouse #2 and #5 showed curvilinear dark signal intensity in the periphery of the mass in 6 and 24 hr post-injection images, which were not present in 48hr images. Mouse #5 also showed very dark signal intensity in the side of Ad-hFTH at 6 and 24 hr post-injection, which then disappeared at 48 hr.

Next, *in vitro* tube imaging by adenoviral FTH in U87MG cells was obtained which presented with darker signal intensity in high concentrations of Fe (Fig. 6). When applied to an *in vivo* glioma model, axial T2* images showed a faint hypo-intense lesion within the tumor on day 1 (Fig. 7). Hypo-intense areas within tumor were obviously detected four days after adenoviral injection. From serial MRI of mice with injection of Ad-Mock and Ad-hFTH, T2 and T2* images of mouse brain were acquired for six days (Fig. 8). Dark signal intensity at periphery of the Ad-hFTH tumor appeared at day 1 post-injection, which was distinct with time, and more apparent in T2* images. There was no signal change around the Ad-Mock tumor, with the exception of a linear low signal intensity suggestive of the injection site. Taken together, these data suggest the potential of ferritin as a reporter for MRI in cancer models.

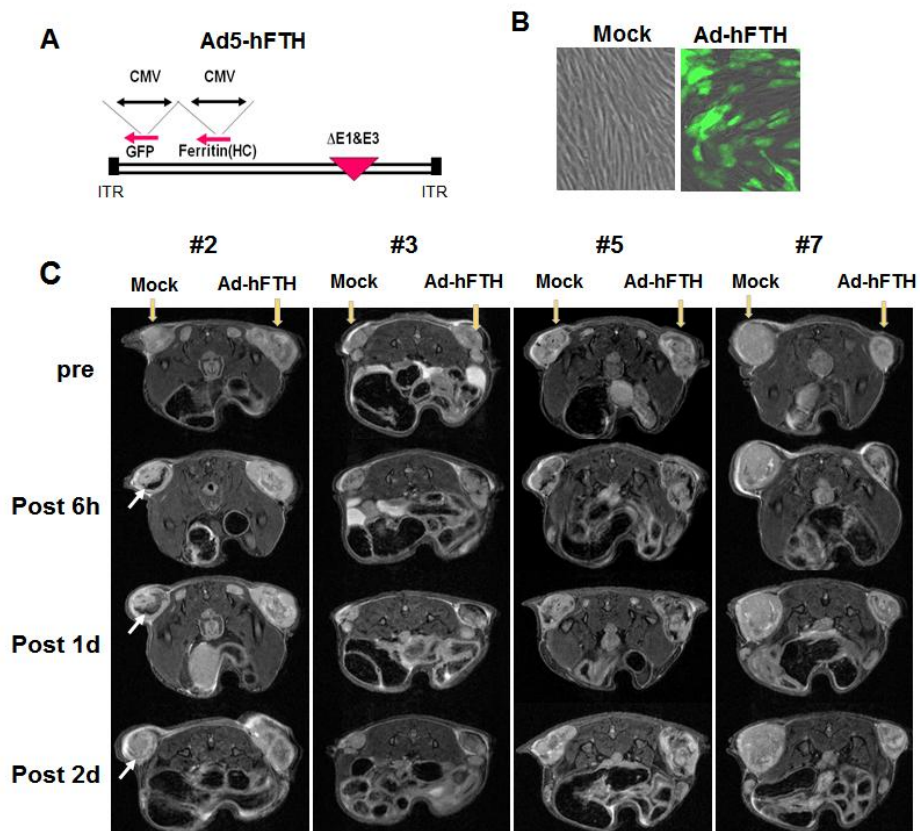


Figure 5. Magnetic resonance imaging (MRI) of ferritin as a reporter in a HCT116 subcutaneous tumor model. (A) Schematic diagram of hFTH expressing an adenoviral vector with the Ad5 backbone and E1/E3 deletion containing the CMV promoter. The adenoviral vector was designed so that GFP expression was able to reflect adenoviral transduction. Abbreviations: CMV, promoter Cytomegalovirus; ITR, Inverted terminal repeat sequences; GFP, Green fluorescence protein; HC, Heavy chain; hFTH, human ferritin heavy chain. (B) GFP-positive cells indicate hFTH expression at 48hr after adenovirus infection in U87MG cells. (C) Ad-FTH was intratumorally injected. Mock viruses were also intratumorally injected into the other side of the tumor mass. T2-weighted MR images showed low signal intensity within the tumor 6hr post-injection at the Ad-FTH injected side, and became distinct with time. The dark curvilinear signal intensity on the Mock injected side (white arrow) disappeared two days post-injection.

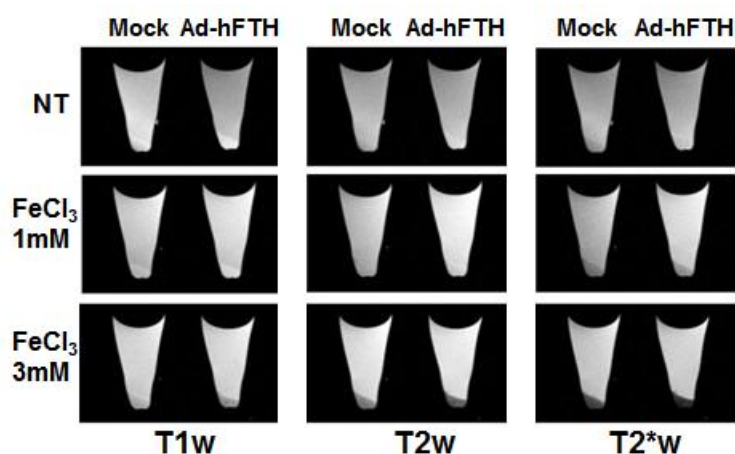


Figure 6. Ferritin-induced magnetic resonance (MR) contrast effect *in vitro* in U87MG cells. To prepare cell pellets for MR imaging, U87MG cells (3×10^6) were infected with Mock and Ad-hFTH (2×10^8 PFU) for 48 hr under complete culture conditions. FeCl₃ was added at indicated concentrations during infection. After incubation, all cells were pelleted by centrifugation and washed with PBS three times, followed by MRI measurements of cell pellets transferred to strip tubes. Abbreviations: T1w, T1-wighted; T2w, T2-wighted T2*w, T2*-wighted. Experimental detail is described in the Materials and Methods.

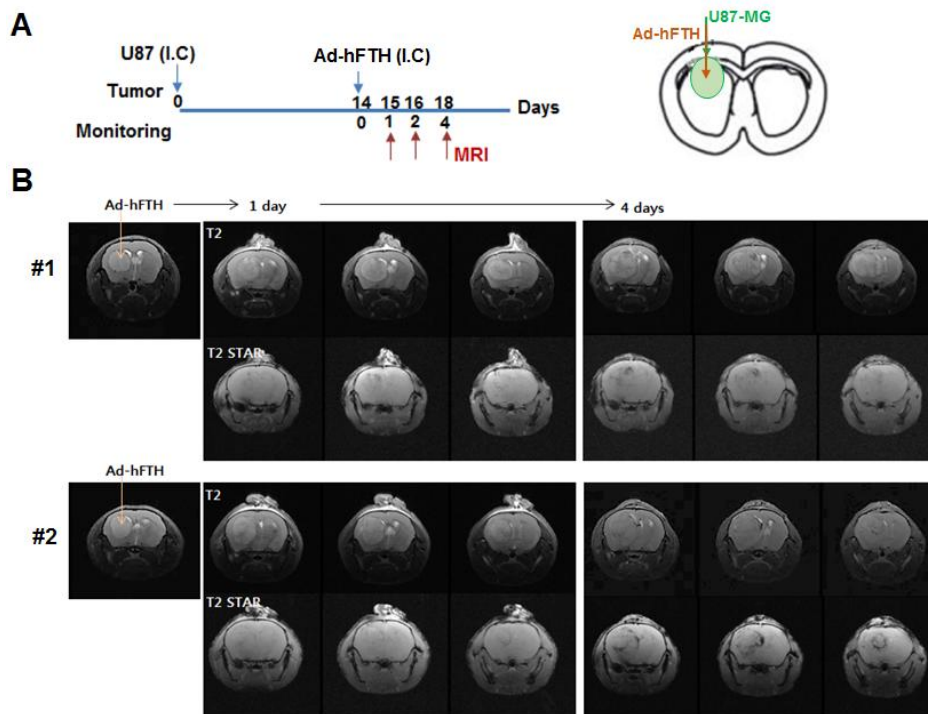


Figure 7. Brain magnetic resonance images in a glioma mouse model infected with Ad-FTH. (A) Experimental scheme using a U87 tumor model. Abbreviations: I.C, *intracranial*. (B) Axial images of animal models showed a faint hypointense lesion within the tumor on day 1 (#1). Hypointense areas within the tumor are evident at day 4. Multifocal hypointense foci within the tumor and a hypointense rim (#2). The image contrast of T2-weighted images showed relatively weak contrast to T2*-weighted images, however, the image contrast of T2-weighted images was strong enough to detect the tumor.

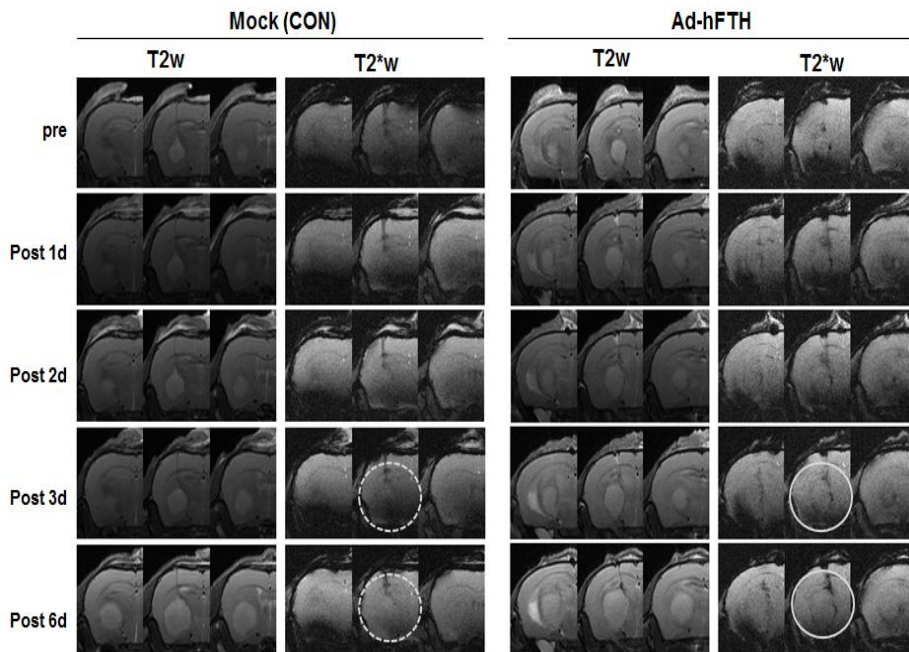


Figure 8. Serial magnetic resonance imaging (MRI) of a glioma with Ad-hFTH. From serial MRI of mice after injection of Mock and Ad-hFTH, T2 and T2* images of mouse brain were acquired for six days. Dark signal intensity at the periphery of the Ad-hFTH tumor appeared at day 1 post-injection, which was distinct with time, and more apparent in T2*w images. T2*w axial images show a hypo-signal peripheral rim (white circle) around the tumor three days after injection of Ad-hFTH. There was no signal change around the Mock-treated tumor, with the exception of linear low signal intensity suggestive of the injection site (white dotted circle).

IV. DISCUSSION

This study showed that negative T2 and T2* contrast enhancement can be identified in a FTH-expressing cancer mouse model by adenoviral gene delivery, suggesting that ferritin could be a potential candidate for a MR reporter gene in cell tracking imaging.

Cell tracking MRI is a common requirement in biomedical research, ranging from cancer models to cardiac and neurological disease. Since MRI can provide anatomical and functional information simultaneously, the application of MRI has been increased to the imaging of cell survival and proliferation, and a number of reporter gene methods have been developed for this purpose¹⁵. A more widely examined option in the search of MRI reporter genes has involved the family of proteins responsible for maintenance of iron homeostasis. Free iron is highly reactive, as it catalyzes the Fenton reaction to generate hydroxyl radicals. Thus, the level of free iron in cells is firmly controlled by reciprocal suppression of transcription, and an increase in protein stability of iron uptake via the transferrin receptor (TfR) and iron storage in ferritin through specific iron responsive elements. TfR was the first potential candidate of reporter genes to be evaluated; however, TfR-associated contrast was markedly enhanced by using transferrin labeled contrast media^{3, 16}. An alternative approach was demonstrated for *in vivo* adenoviral-mediated infection of neurons to overexpress ferritin^{16, 17}. In addition, several previous studies from multiple laboratories have used the overexpression of ferritin^{17, 21, 22}.

Contrast agents based on superparamagnetic particles are in clinical development. The relaxivities are frequently used to give an idea of their efficacy; however, these parameters can only be used if they are concentration independent²³. Usually, superparamagnetic iron oxide nanoparticles can be utilized to label cells. In conventional MRI with superparamagnetic particles,

the signal voids arising from the field distortions lead to negative contrast, which is not desirable, as the detection of cells can be masked by native low signal tissue. Additionally, it is difficult to quantify the concentration of the superparamagnetic particles.

In order to overcome the negative contrast from the superparamagnetic iron oxide nanoparticles, many imaging techniques have been developed, including positive contrast imaging, susceptibility-weighted imaging, and susceptibility mapping^{24,25}. In positive contrast imaging, the signal is obtained from off-resonance spins around the superparamagnetic iron oxide nanoparticles. The strong field distortion from the superparamagnetic particles can be detected by exciting the off-resonance spins. For susceptibility-weighted imaging and susceptibility mapping, complicated bundles of image post-processes such as a phase map are used after the MRI scan. Many studies have reported on more accurate maps and faster calculations. The algorithms for image post-processing are still controversial among many research groups. Due to the complexity and controversy of the quantification, superparamagnetic particle quantification was not applied to the analysis of the animal images in this study.

Meanwhile, for long-term cell tracking, the establishment of a stable cell line was predominantly attempted using lentiviral or retroviral expression systems. However, there were some limitations to the use of lentiviruses in this study. One major limitation was that infected cancer cells showed irregular expression levels due to the wide range of copy number variants and increased population of dead cells because of high-titer lentivirus-induced toxicity, and thereby it required a sorting step and amplification periods for *in vivo* inoculation. The gene delivery vehicle, which is a determinant of transduction efficiency and safety, is a key element for successful expression. The serotype 5 adenovirus is the most favored gene delivery vehicle, which is currently being used

extensively in more than 100 cancer gene therapy clinical trials across the world; adenoviruses have the advantage of being able to transduce in both dividing and non-dividing cells, amplify in high-titer easily, and they do not integrate into the host genome²⁶. The adenoviral vector used in this study was designed to monitor transduction efficiency through GFP expression, although the GFP expression level is not capable of reflecting hFTH expression perfectly, like the hFTH-IRES-GFP system. The commercially available adenovirus used in this study, the construction of which is shown in Fig. 5A, is able to generate high-titer adenovirus for *in vivo* use in small volumes, and minimize batch variation. The hFTH expressed by the adenovirus triggered Fe uptake around inflammatory regions such as those in atherosclerosis or cancer. Like macrophages, stem cells are known to have tumor tropism as well as wound-related inflammation. Many people have suggested that mesenchymal stem cells may be useful as a gene delivery tool in cancer therapy. Gene delivery requires a tracking system to monitor targeting efficiency and predict therapeutic efficacy. The reporter gene system using ferritin could be a multi-detection system for tracking of delivery vehicle location, cancer region, and stem cell fate, if adopted in stem cell-mediated gene delivery²⁷.

V. CONCLUSION

Through cellular level investigation and *in vivo* experiments using animal models, this study strongly suggests the effectiveness of ferritin as an endogenous MR contrast agent and as a potential reporter gene, which is capable of maintaining cell labeling stability and cellular safety.

REFERENCES

1. Youn H. CJ. Reporter Gene Imaging AJR 2013;201:W206-W14.
2. Brader P SI, Blasberg RG. Noninvasive molecular imaging using reporter genes. J Nucl Med 2013;54:167-72.
3. Weissleder R, Moore A, Mahmood U, Bhorade R, Benveniste H, Chiocca EA, et al. In vivo magnetic resonance imaging of transgene expression. Nat Med 2000;6:351-5.
4. Kang HW, Josephson L, Petrovsky A, Weissleder R, Bogdanov A, Jr. Magnetic resonance imaging of inducible E-selectin expression in human endothelial cell culture. Bioconjug Chem 2002;13:122-7.
5. Zhao M, Beauregard DA, Loizou L, Davletov B, Brindle KM. Non-invasive detection of apoptosis using magnetic resonance imaging and a targeted contrast agent. Nat Med 2001;7:1241-4.
6. Artemov D, Mori N, Okollie B, Bhujwala ZM. MR molecular imaging of the Her-2/neu receptor in breast cancer cells using targeted iron oxide nanoparticles. Magn Reson Med 2003;49:403-8.
7. Huh YM, Jun YW, Song HT, Kim S, Choi JS, Lee JH, et al. In vivo magnetic resonance detection of cancer by using multifunctional magnetic nanocrystals. J Am Chem Soc 2005;127:12387-91.
8. Jun YW, Huh YM, Choi JS, Lee JH, Song HT, Kim S, et al. Nanoscale size effect of magnetic nanocrystals and their utilization for cancer diagnosis via magnetic resonance imaging. J Am Chem Soc 2005;127:5732-3.
9. Czernin J, Phelps ME. Positron emission tomography scanning: current and future applications. Annu Rev Med 2002;53:89-112.
10. Graves EE, Weissleder R, Ntziachristos V. Fluorescence molecular imaging of small animal tumor models. Curr Mol Med 2004;4:419-30.

11. Bulte JW, Kraitchman DL. Iron oxide MR contrast agents for molecular and cellular imaging. *NMR Biomed* 2004;17:484-99.
12. Song HT, Choi JS, Huh YM, Kim S, Jun YW, Suh JS, et al. Surface modulation of magnetic nanocrystals in the development of highly efficient magnetic resonance probes for intracellular labeling. *J Am Chem Soc* 2005;127:9992-3.
13. Lee JH, Huh YM, Jun YW, Seo JW, Jang JT, Song HT, et al. Artificially engineered magnetic nanoparticles for ultra-sensitive molecular imaging. *Nat Med* 2007;13:95-9.
14. Pawelczyk E, Arbab AS, Pandit S, Hu E, Frank JA. Expression of transferrin receptor and ferritin following ferumoxides-protamine sulfate labeling of cells: implications for cellular magnetic resonance imaging. *NMR Biomed* 2006;19:581-92.
15. Gilad AA, Winnard PT, Jr., van Zijl PC, Bulte JW. Developing MR reporter genes: promises and pitfalls. *NMR Biomed* 2007;20:275-90.
16. Genove G, DeMarco U, Xu H, Goins WF, Ahrens ET. A new transgene reporter for in vivo magnetic resonance imaging. *Nat Med* 2005;11:450-4.
17. Cohen B, Ziv K, Plaks V, Israely T, Kalchenko V, Harmelin A, et al. MRI detection of transcriptional regulation of gene expression in transgenic mice. *Nat Med* 2007;13:498-503.
18. Uchida M, Terashima M, Cunningham CH, Suzuki Y, Willits DA, Willis AF, et al. A human ferritin iron oxide nano-composite magnetic resonance contrast agent. *Magn Reson Med* 2008;60:1073-81.
19. Carrondo MA. Ferritins, iron uptake and storage from the bacterioferritin viewpoint. *EMBO J* 2003;22:1959-68.
20. Gossuin Y, Muller RN, Gillis P. Relaxation induced by ferritin: a better understanding for an improved MRI iron quantification. *NMR Biomed* 2004;17:427-32.

21. Choi SH, Cho HR, Kim HS, Kim YH, Kang KW, Kim H, et al. Imaging and quantification of metastatic melanoma cells in lymph nodes with a ferritin MR reporter in living mice. *NMR Biomed* 2012;25:737-45.
22. Kim HS, Joo HJ, Woo JS, Choi YS, Choi SH, Kim H, et al. In vivo magnetic resonance imaging of transgenic mice expressing human ferritin. *Mol Imaging Biol* 2013;15:48-57.
23. T B-G. Ferrimagnetic susceptibility contrast agents. *Acta Radiol Suppl* 1993;387:1-30.
24. Eibofner F, Steidle G, Kehlbach R, Bantleon R, Schick F. Positive contrast imaging of iron oxide nanoparticles with susceptibility-weighted imaging. *Magn Reson Med* 2010;64:1027-38.
25. de Rochefort L1 LT, Kressler B, Liu J, Spincemaille P, Lebon V, Wu J, Wang Y. Quantitative susceptibility map reconstruction from MR phase data using bayesian regularization: validation and application to brain imaging. *Magn Reson Med* 2010;63:194-206.
26. Ghosh SS GP, Ramesh A. Adenoviral vectors: a promising tool for gene therapy. *Appl Biochem Biotechnol* 2006;133:9-29.
27. D'souza N RF, Golinelli G, Grisendi G, Spano C, Candini O, et al. Mesenchymal stem/stromal cells as a delivery platform in cell and gene therapies. *BMC Med* 2015;12:186.

ABSTRACT(IN KOREAN)

동맥경화증과 종양마우스모델에서 페리틴을 이용한
세포추적자기공명영상

<지도교수 서 진 석>

연세대학교 대학원 의학과

이 찬 화

분자영상은 생체 내 분자 혹은 세포수준에서 일어나는 현상들을 실시간 영상을 통해 좀 더 쉽고 분명하게 이해할 수 있게 하는 매우 혁신적인 영상분야이다. 분자영상 영역의 적용 분야 중 자기공명영상은, 세포 표지를 통해 이동, 증식 및 분화를 추적할 수 있고, 표지하는 세포의 종류에 따라 종양 및 염종의 진단 및 치료효과를 검정하는 데에도 이용될 수 있다. 우수한 조직대조도의 강점을 갖는 자기공명영상은 상대적으로 조직민감도가 낮다는 한계점을 극복하기 위하여 조영제를 사용하게 되는데, 생체 내 조영제 농도의 희석, 표지의 불안정성 및 세포 독성 등의 문제점이 유발되는 경우가 많아, 보다 안전하고 효율적인 세포표지방법의 개발이 요구되고 있다. 리포터유전자를 이용한 방법은 상기 한계점들을 극복할 수 있는 한 방법으로서 제안되고 있다. 페리틴은 생체 내에 존재하는 철 결합

단백질의 일종으로, 세포 외부로부터 유입된 철 이온을 내부에 축적함으로써 내재적 자성을 띠어 자기공명영상에서 T2 조영 효과를 보일 수 있으므로 세포추적을 위한 자기공명영상용 조영제로서 좋은 후보라 할 수 있다. 본 연구에서는 동맥경화증과 종양 마우스 모델에서 페리틴을 이용한 대식세포 및 종양세포의 추적을 통해 페리틴의 조영제 적용 및 리포터 유전자로서의 활용가능성을 알아보고자 하였다. 현재 사용되고 있는 T2 조영제인 페리텍스와의 비교실험에서, 페리틴의 자기공명이완율 (R2)은 페리텍스의 약 50%로(페리텍스 vs 페리틴 = $0.00298 \text{ ml/Fe } \mu\text{g } 1/\text{s}$ vs $0.00159 \text{ ml/Fe } \mu\text{g } 1/\text{s}$) 계산되어 상대적으로 낮으나, 자기공명조영제로의 사용은 충분하였다. 페리틴을 배양시켜 표지한 대식세포주 Raw264.7 역시, 세포펠렛 (cell pellet) 영상으로부터 T1 과 T2조영효과를 보였으며, 이를 아포E녹아웃(*ApoE*^{-/-}) 마우스에 정맥 주사한 24시간 후 얻은 생체영상에서 대동맥궁 혈관벽의 음성 조영 효과를 관찰할 수 있었다. 이로써 페리틴으로 표지된 세포의 추적을 통해 생체 내 염증의 진단이 가능함을 알 수 있었다. 페리틴에 의한 조영 효과가 검증되었으므로, 이후 리포터 유전자로서의 활용가능성을 검증하고자 하였으며 이를 위한 실험에서는 아데노바이러스 기반의 발현 시스템을 이용하였다. 먼저, 대장암 세포주인 HCT116을 이용하여 제작한 피하종양모델에 대조군인 Mock과 실험군인 Ad-hFTH (adenoviral human ferritin heavy chain)를 각각 주사하였다. 주사 후 2일마다 T1 & T2강조영상을 얻었으며, 주사 후 2일째 영상에서 종양 내 음성 조영 부분이 나타난 후, 4일째 영상에서 종양증강부분이 더욱 뚜렷하게 관찰되었다. 해당 조직에 시행한 Prussian Blue 염색 결과, 음성 조영 증강 부분과 철 흡수 영역이 중첩되므로 페리틴 유전자 발현

에 의한 조영 효과 임을 확인하였다. 철의 농도가 종양영역 내에서 높아지는 환경적 특성을 고려하여, 뇌암 세포주인 U87MG에 Ad-hFTH를 감염시켜 페리틴 발현을 유도한 후 배양 환경에 FeCl_3 의 농도를 각각 1 mM과 3 mM로 첨가하여 세포 펄스 자기공명영상을 시행하였을 때, 철의 농도가 높을수록 음성 조영 증강효과가 더 강하게 나타남을 확인하였다. $T2^*$ 강조영상을 통한 페리틴의 음성 조영 효과를 재확인하기 위하여, U87MG 세포를 마우스 뇌에 정소 이식하여 뇌종양 모델을 제작한 후, 종양 내로 Ad-hFTH를 주사하여 1일째부터 6일째까지의 $T1$, $T2$ & $T2^*$ 강조영상을 동시에 획득하였다. 주사 후 2일째부터 $T2$ 와 $T2^*$ 강조영상에서 종양의 변연부에 음성 조영 효과가 관찰되기 시작하며, 이는 6일째까지 유지되는 양상을 보였다. 결론적으로, 본 연구는 세포 수준에서의 조사와 동물 모델을 이용한 생체 적용 실험을 통하여, 세포 표지의 안정성 및 세포 안전성을 충족시킬 수 있는, 자기공명영상을 위한 내재적 조영제로서의 페리틴의 활용 가능성을 강력히 제시하고 있다.